CFD modelling of lab-scale anaerobic digesters to determine experimental sampling locations

Rebecca Sindall[1], John Bridgeman[1] and Cynthia Carliell-Marquet[1]

[1] School of Civil Engineering, University of Birmingham, UK.

rcs587@bham.ac.uk

Abstract

Literature suggests that microbiological communities in anaerobic digesters are damaged at high mixing speeds, reducing biogas production. This paper uses CFD to model a lab-scale mechanically-mixed digester and explore the patterns of turbulent kinetic energy at different mixing speeds. Results using four turbulence models are compared to PIV results and it is found that realisable k-ε is best at predicting digester flow patterns. It is shown that in order to assess the effect of mixing upon the microbiology of the digester, microbial samples should be taken from the impeller region, as well as regions above and below the impeller.

1 Introduction

Each day, the UK water industry collects, treats, and returns to the environment over 10 billion litres of waste water at over 9000 wastewater treatment sites. Sewage sludge is a by-product of this treatment process. Anaerobic digestion (AD) is the most common method of stabilising the sludge before it is disposed of to land. Biogas, the main by-product of AD, can be used as a renewable source of heat and power through the use of combined heat and power units. Thus, increasing the biogas production of an anaerobic digester becomes desirable. Mixing in anaerobic digesters is necessary to bring bacteria in the biomass and food sources in the sludge together so that sludge stabilisation can occur (USEPA, 1976). However, the effects of mixing on biogas production are not clear, though there is a growing body of literature that suggests that a low level of mixing is beneficial (Kaparaju et al., 2008, Stroot et al., 2001). It is hypothesised that this is because high levels of turbulence at high mixing speeds are detrimental to methane-producing bacteria (Hoffman et al., 2008). In this work, CFD simulations of a lab-scale mechanically-mixed digester are used to identify areas of high and low turbulence within digesters mixed at different speeds. This allows future experimental work to identify appropriate sampling locations for the study of microbiological communities present in areas of high and low turbulence. This will allow a better understanding of the link between mixing and biogas production.

2 Methodology

2.1 Model geometry

The CFD model is of a cylindrical vessel with a four-bladed flat impeller and four baffles spaced equally around the vessel wall. The geometry of the vessel and the detail of the impeller are shown in Figure 1. The digester has a diameter of 200 mm and a height of 200mm. The impeller has a

diameter of 90 mm, height of 20 mm, and blade thickness of 8 mm. It is located so that the impeller centreline is 60 mm above the base of the digester. The baffles are 10 mm thick and extend 10 mm from the vessel side.

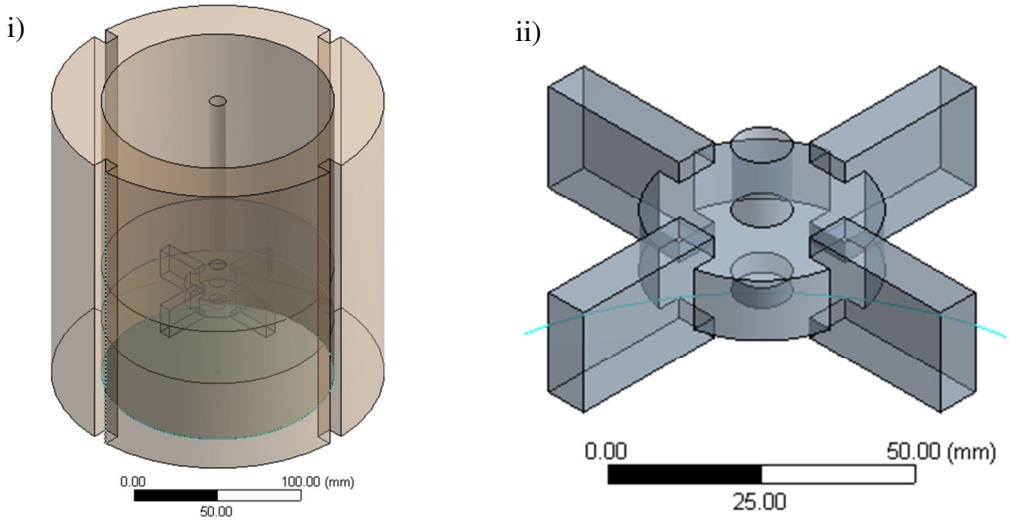

Figure 1– Geometry of i). the digester vessel and ii). the impeller

2.2 *Numerical method and boundary conditions*

Commercial CFD software, ANSYS Fluent 13.0 (ANSYS-Fluent, 2010a) was used to create the digester model. The geometry and mesh were created using ANSYS DesignModeler and ANSYS Meshing in ANSYS Workbench 13.0 (ANSYS-Fluent, 2010b).

The simulations were run using a second-order upwind discretisation scheme for the convection terms whilst the pressure terms were discretised using a central differencing scheme. The use of a second order convection scheme allows for better resolution of the gradients which in turn gives more accurate solutions than a first-order scheme. However, second-order schemes can take significantly longer to run. Following current best practice, simulations were run using a first-order convection scheme until they were partially-converged and then a second-order convection scheme was applied to reach a fully-converged solution. The semi-implicit method for pressure-linked equations (SIMPLE) (Patanker and Spalding, 1972) is used for de-coupling pressure and velocity.

A sliding mesh (SM) is used in order to capture any unstable flows as the level of rotor-stator interaction is unknown. With the SM method, the vessel is split into two regions, the impeller region and the bulk region. The mesh within the impeller region rotates at a rotational velocity equal to that of the impeller, whilst the mesh within the bulk region remains stationary. The momentum equations are solved across the mesh for each time step, and at the end of the time step, the impeller region slides past that of the bulk region. For this to be possible, the interface between the two regions must be rotationally symmetrical and non-conformal. At the end of each time step, the non-conformal interfaces are updated to reflect the new positions of the two zones relative to one another. This method allows the model to predict unsteady flows as they occur.

All of the walls of the digester, including the base and the impeller blades were specified using a no slip condition. In order to accurately capture the boundary layer, 5 prism layer cells are used on all surfaces that are considered as walls, with a growth rate of 1.2 and the thickness of the first cell being 0.1 mm. As the maximum $y+$ in the digester is 1.46, a wall function is not necessary. The liquid free surface was modelled as a symmetry plane.

The non-Newtonian fluid model used was calculated from viscosity measurements of the sludge used in the experimental work, carried out using a Couette viscometer (Fann Model 35). The model uses a density of 965 kg/m^3 and follows a non-Newtonian power law model, $\eta = k\gamma^n$, with consistency index, k = 0.0788 Pa-s$^{0.8088}$, power law index, n = 0.8088 and allowable viscosity range of 0.02–0.035 kg/m-s. A non-Newtonian power law viscosity model was chosen as it has been successfully employed to describe the rheological properties of sewage sludge previously (Seyssiecq et al., 2003) and is considered to be a robust but straightforward model.

2.3 Computational mesh

The unstructured hexahedral mesh was generated using ANSYS Meshing in Workbench 13.0 (ANSYS-Fluent, 2010b). The Grid Convergence Index (GCI) (Roache, 1998) is a simple method to report grid convergence without being limited to doubling the number of cells in each consecutive grid. This allows the grid density to be analysed to provide an indication of error bands. Velocity magnitude values were extracted for 500 individual points in the flow field, and the GCI was calculated as:

$$GCI = F_s \frac{e_{rms}}{r^2 - 1}$$

$$e_{rms} = \sqrt{\frac{\sum_{m=1}^{750} \left|\left(u_{m,1} - u_{m,2}\right)/u_{m,2}\right|^2}{500}}$$

$$r = \left(\frac{h_2}{h_1}\right)^{1/3}$$

where u_m is velocity magnitude at point m, h is the number of cells in the mesh and subscripts 1 and 2 refer to coarse and fine mesh respectively. A factor of safety of F_s = 1.25 was applied in accordance with published recommendations for the comparison of multiple grids (Roache, 1998).

Five grid densities were tested: 402,000, 603,000, 966,000, 1,409,000 and 2,347,000. Taking the coarsest mesh as a baseline, GCIs were calculated for the finer grids as 9.6 % (603,000), 7.5 % (966,000), 5.9 % (1,409,000) and 5.7 % (2,347,000). From this, it can be seen that the solutions from the two finest grids approach solution convergence. Whilst the two grids fall slightly outside the 95 % confidence interval, the increase in computing time when increasing the mesh density from 1,409,000 to 2,347,000 was not considered to reflect a corresponding increase in the accuracy of the results and as such the 1,409,000 cell grid will be used to calculate flow patterns in the digester. As such, error bars of 6 % can be attached to the results of the simulations undertaken.

3 Results

3.1 Model validation and turbulence model selection

The results from a number of simulations which made use of various turbulence models were compared to the results of particle image velocimetry (PIV) experiments carried out in a clear plastic replica digester mixing 0.5 g/l carboxymethyl cellulose (CMC) solution at 100 rpm. The turbulence models tested were the realisable *k-ε*, standard *k-ω*, SST *k-ω* and Reynolds Stress Model.

Figures 2 and 3 show the *u* and *v* velocities along a line at *r/R* = 0.6 with results taken from PIV and CFD simulations. It can be seen that all four turbulence models are able to recreate the general shape

of the *u* and *v* velocity plots for the PIV data. For all of the turbulence models the peak *u* velocities in the impeller region are predicted to be slightly higher than the peak demonstrated by the PIV data. The magnitude of the peak *u* velocity is best predicted by the SST *k-ω* model and the Reynolds Stress Model. Both the standard *k-ω* and the realisable *k-ε* models underestimate the magnitude of the peak. Below the impeller, all four of the turbulence models follow the same curve and all four underestimate the magnitude of the *u* velocity. There are significant differences between the four turbulence models considered above the impeller. Unfortunately, due to the limited frame used in the PIV data, the behaviour of the sludge in the top third of the digester was not monitored and no comparison between the CFD and PIV data can be made. In the area directly above the impeller the *u* velocities predicted by the realisable *k-ε* model are closest to the shape and magnitude of the PIV data. Whilst parts of this curve are well followed by the standard *k-ω* and the SST *k-ω* models, the Reynolds Stress Model does not predict the *u* velocities well in this area.

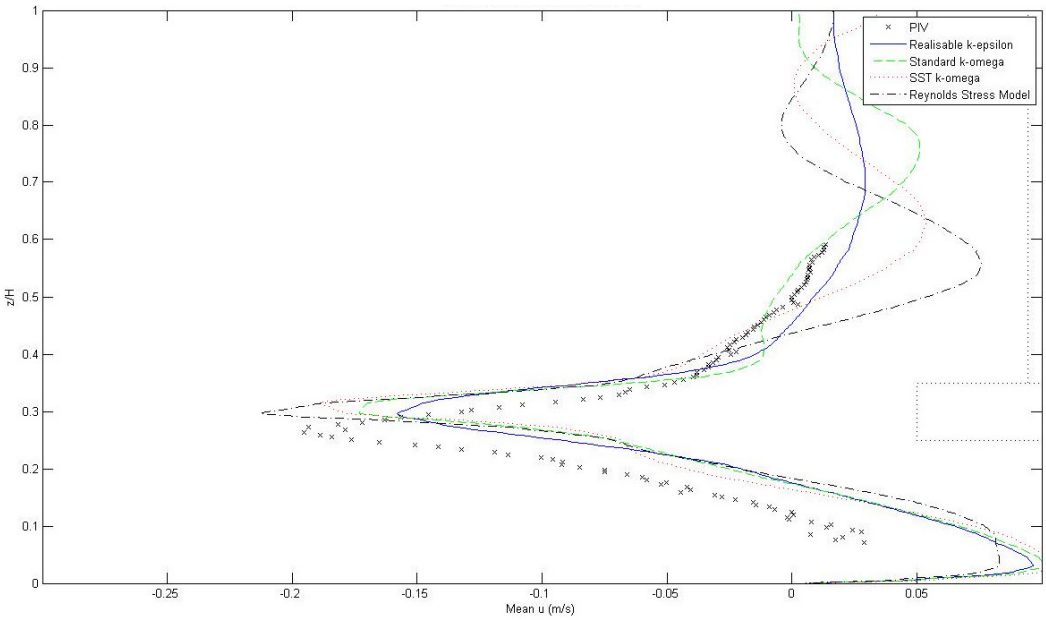

Figure 2 – *u* velocities along a line at $r/R = 0.6$ modelled using four different turbulence models, as compared to results from PIV

As for the *u* velocities, the location and magnitude of peak *v* velocities are well predicted by the CFD simulations with the standard *k-ω*, SST *k-ω* and Reynolds Stress Models all predicting the magnitude of the peak below the impeller very well despite placing it slightly higher in the digester than it is seen to occur from the PIV data. The realisable *k-ε* model is better at locating the peak, though it underestimates the magnitude. This is also true when considering the peak above the impeller. This is well-located by the SST *k-Ω* and Reynolds Stress Models as well, though these models overestimate the magnitude of the peak. The standard *k-Ω* model underestimates the magnitude of this peak but predicts a wider peak than is identified by the PIV data. The realisable *k-ε* model predicts the uppermost PIV data points with remarkable accuracy.

From the *u* and *v* velocity PIV data, the turbulent kinetic energy was calculated and compared to the turbulent kinetic energy predicted by the CFD simulations as shown in Figure 4. Whilst all four of the turbulence models are able to predict the location of the peak turbulent kinetic energy, none of the models predict the magnitude of the peak well. The best of the models is the realisable *k-ε* model which predicts approximately 65 % of the peak magnitude. The other three models predict less than 15 % of the peak magnitude.

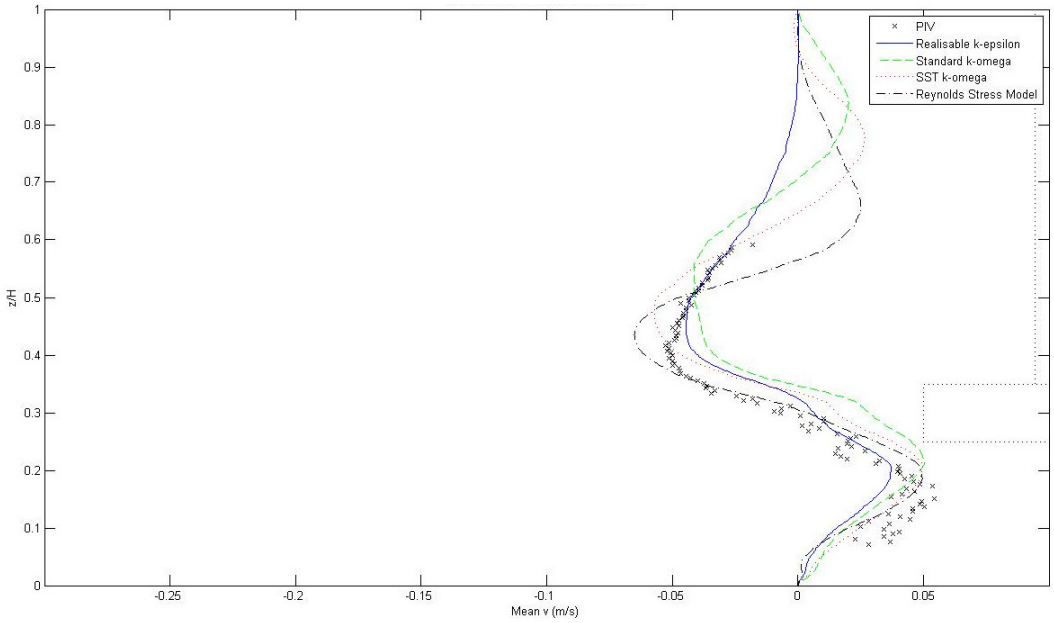

Figure 3 – *v* velocities along a line at *r/R* = 0.6 modelled using four different turbulence models, as compared to results from PIV

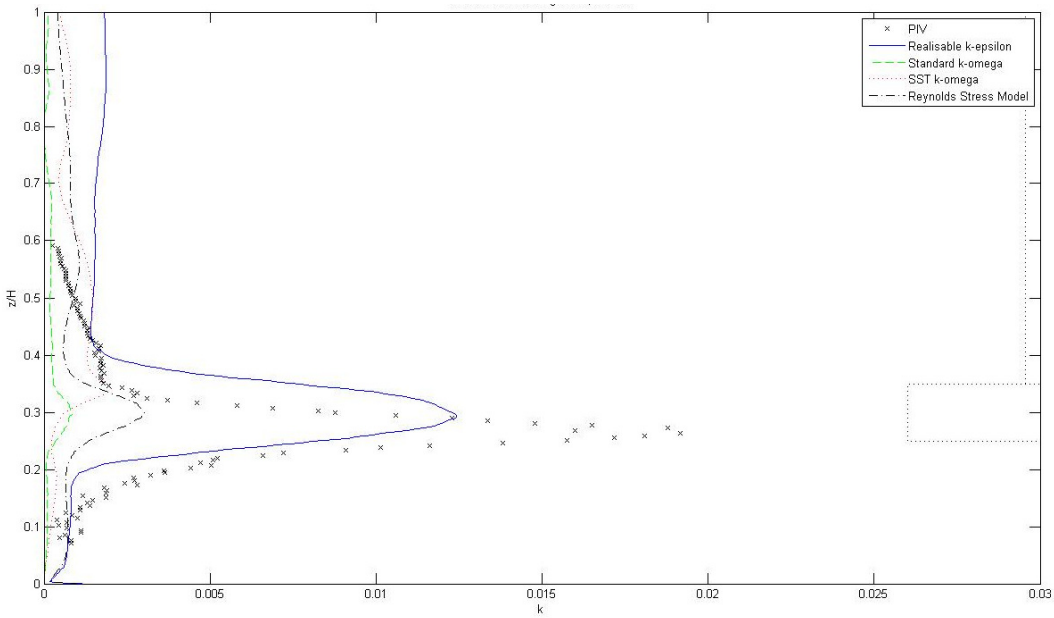

Figure 4 – Turbulent kinetic energy, *k*, along a line at *r/R* = 0.6 modelled using four different turbulence models, as compared to results from PIV

Whilst the realisable *k-ε* model underestimates the peak magnitudes of both velocity and turbulent kinetic energy, it appears to be the best fit to the PIV data. It is also the best at predicting the turbulent kinetic energy. As such, all further results are based on simulations which make use of the realisable *k-ε* model.

i).

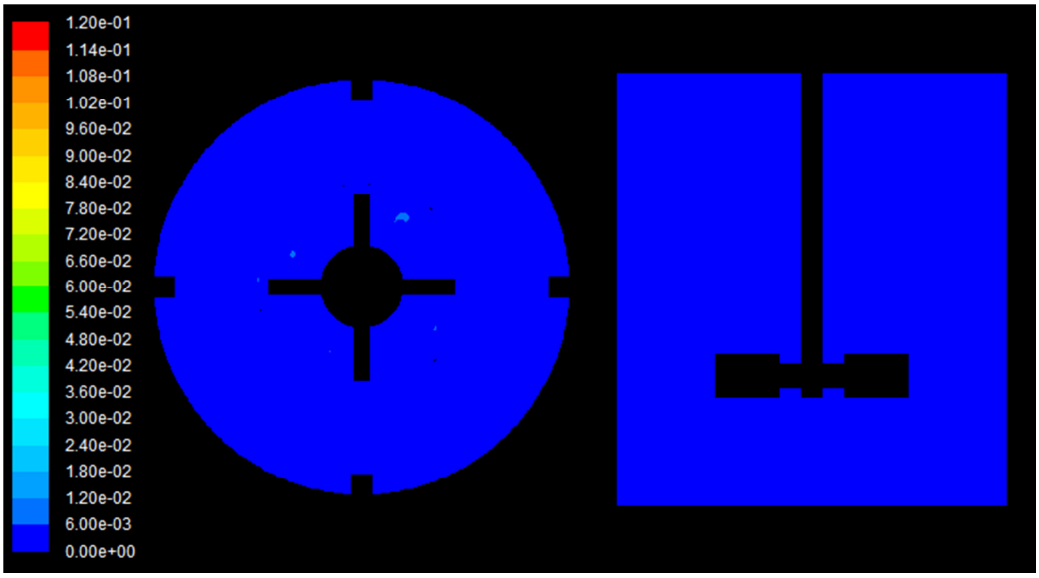

ii).

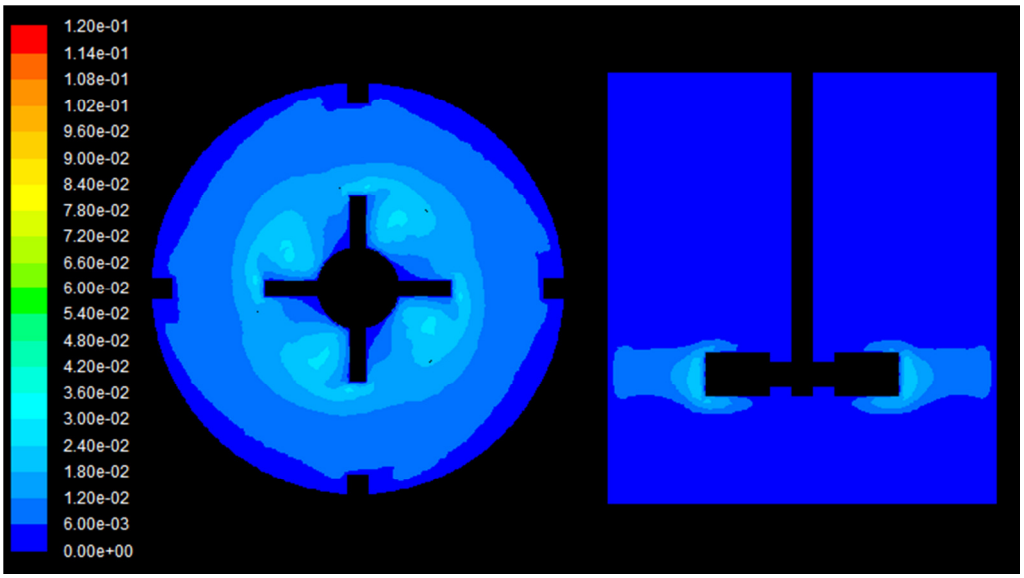

iii).

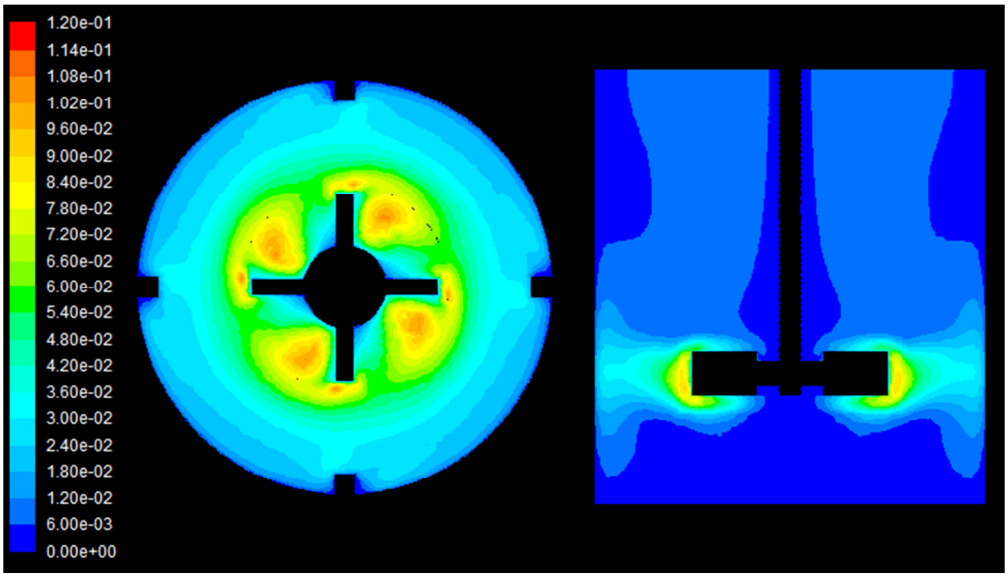

Figure 5 – Contour plots of turbulent kinetic energy for digesters mixed at i). 50 rpm, ii). 100 rpm and iii). 200 rpm

3.2 Turbulent kinetic energy

Turbulent kinetic energy (TKE) is the mean kinetic energy per unit mass. It is the result of fluid shear, friction or buoyancy and therefore may be considered as an indication of the impact of turbulence on flocs and microbial communities in the digester. As TKE is calculated from a scalar transport equation, it is likely that the exact values predicted by Reynolds-averaged Navier-Stokes (RANS) CFD models as used here will be inaccurate. The accuracy of these results could be improved by using a large eddy simulation (LES) model. However, the contours and relative magnitudes across the vessel predicted by RANS simulations in this work are still of interest. The k-ε model used in these simulations models the TKE based on the assumption that turbulence is isotropic. In scenarios where anisotropic turbulence dominates, it is expected that this will lead to the over-prediction of TKE, although this is not the case when comparing the model to the PIV experiments discussed above.

Figure 6 shows the TKE contours in the digester at mixing speeds of 50, 100 and 200 rpm respectively. At a mixing speed of 50 rpm, there is virtually no predicted TKE. At 100 rpm and 200 rpm, there are differences in the magnitude of the TKE but the contour patterns are similar. Notably, and unsurprisingly, the highest levels of TKE appear in the impeller region, with virtually no TKE predicted above and below the impeller. The magnitude of TKE at the tips of the impeller blades and in the recirculation regions in the wake of the blades is a magnitude higher than in the bulk of the digester. This clearly demonstrating that it is in the impeller region that the turbulence experienced is at its highest.

3.3 Turbulent intensity

The turbulence intensity, I, is often used as a non-dimensional measure of the level of turbulence. It is defined mathematically as:

$$I = \frac{\sqrt{\frac{2}{3}k}}{u}$$

where k is turbulent kinetic energy and u is the mean velocity.

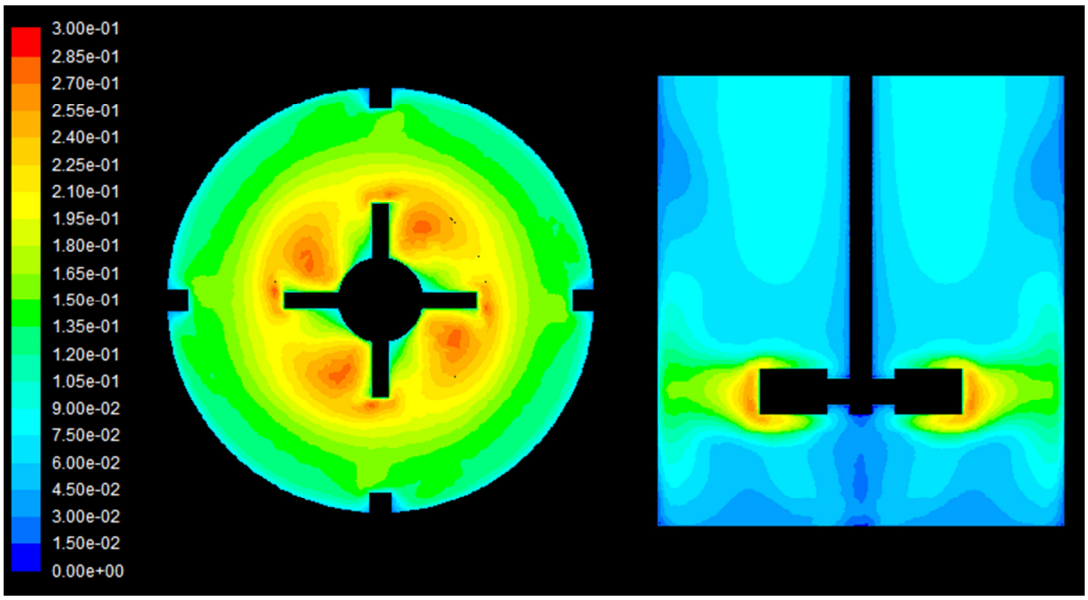

Figure 6 – Contour plots of turbulence intensity for a digester mixed at 200 rpm

The mean velocity was selected as the tip speed of the impeller in order to give a global turbulence intensity. Figure 6 shows an example of the turbulence intensity contours in the digester. By normalising the turbulence intensity by dividing by the tip speed, all of the digesters experience similar contours and turbulence intensity magnitudes. The bulk of the digester experiences very little turbulence, with turbulence intensities of 10 % or lower. However, in the plane of the impeller, the turbulence intensity is significantly higher, with intensities of 10-20 % close to the walls and of 20-30 % in the impeller region. Once again, the highest turbulence intensities are found at the tip of the impeller blades and in the recirculation regions in the wake of the blades.

From this, it can be seen that turbulence intensity varies dramatically across the digester. As such, in order to judge the effects of mixing on microbiological communities, samples would need to be taken from the impeller region as well as from the regions above and below the digester.

4 Conclusions

In this work, a lab-scale anaerobic digester was modelled using a range of turbulence models and compared to PIV experiments. The realisable k-ε model was found to be most capable of accurately predicting the flow patterns brought about by mixing. Using this model, it was found that the highest levels of TKE are found in the impeller region. The magnitude of TKE at the tips of the impeller blades and in the recirculation regions in the wake of the blades was an order of magnitude higher than in the bulk of the digester. As mixing speeds increase, the magnitude of TKE was found to increase correspondingly, giving similar contours of turbulence intensity at all mixing speeds. A more complex model, such as LES, would be required to accurately assess the value of TKE, but this work does demonstrate the relative magnitude of TKE in a digester. This is sufficient to recommend that in order to assess the effects of mixing on microbiological communities, samples should be taken from the impeller region, above the impeller region and below the impeller region.

References

ANSYS-FLUENT 2010a. Fluent 13.0. Lebanon, NH.

ANSYS-FLUENT 2010b. Workbench 13.0. Lebanon, NH.

HOFFMAN, R., GARCIA, M. L., VESVIKAR, M., KARIM, K., AL-DAHHAN, M. H. & ANGENENT, L. T. 2008. Effect of shear on performance and microbial ecology of continuously stirred anaerobic digesters treating animal manure. *Biotechnology and Bioengineering,* 100**,** 38-48.

KAPARAJU, P., BUENDIA, I., ELLEGAARD, L. & ANGELIDAKI, I. 2008. Effects of mixing on methane production during thermophilic anaerobic digestion of manure: Lab-scale and pilot-scale studies. *Bioresource Technology,* 99**,** 4919-4928.

PATANKER, S. V. & SPALDING, D. B. 1972. A calculation procedure for heat, mass and momentum transfer in three-dimensional parabolic flows. *International Journal of Heat and Mass Transfer,* 15**,** 1787-1806.

ROACHE, P. J. 1998. Verification of Codes and Calculations. *American Institute of Aeronautics and Astronautics Journal,* 36**,** 696-702.

SEYSSIECQ, I., FERRASSE, J.-H. & ROCHE, N. 2003. State-of-the-art: rheological characterisation of wastewater treatment sludge. *Biochemical Engineering Journal,* 16**,** 14-56.

STROOT, P. G., MCMAHON, K. D., MACKIE, R. I. & RASKIN, L. 2001. Anaerobic codigestion of municipal solid waste and biosolids under various mixing conditions - I. digester performance. *Water Research,* 35**,** 1804-1816.

USEPA 1976. Anaerobic Sludge Digestion Operations Manual.